JMEPEG (2018) 27:3374–3385
https://doi.org/10.1007/s11665-018-3440-5

1059-9495/$19.00

Notch Sensitivity and Failure Behavior of TiAl and K418 Alloys

R. Cao, J.X. Wen, H.J. Liu, and J.H. Chen

(Submitted November 14, 2017; in revised form May 20, 2018; published online June 5, 2018)

The notch sensitivity of tensile specimens of TiAl and K418 alloys has been investigated, and the notch strength has been quantitatively analyzed. The fracture surface of the specimens has also been observed and analyzed by scanning electron microscopy (JEOL-6700F). By comparing notch rod tensile specimens and special notch rod tensile specimens, it was found that the basic nature, fracture driving force, and fracture criteria of the brittle TiAl alloy and the ductile K418 alloy are different. The final fracture of the K418 alloy is controlled by strain and not by stress, and the specimens do not exhibit notch sensitivity. However, the final fracture of the TiAl alloy is controlled by stress, and the specimens exhibit small notch sensitivity. For the special notch rod tensile specimens, the K418 specimens do not exhibit notch sensitivity. However, for the TiAl alloy, when the notch depth reaches 10% of the specimen diameter, the tensile strength decreases, and when the notch depth reaches 20% of the specimen diameters, the tensile strength sharply decreases.

Keywords fracture, K418 alloys, notch sensitivity, notch strength, TiAl alloys

1. Introduction

Ni-based superalloys are most commonly used for turbocharger turbine wheels; however, their application is hindered by their relatively high densities (around 8 g/cm^3). Comparatively, gamma TiAl has received greater attention as potential material for high-temperature structural applications in the field of turbocharger manufacturing due to its low density (about 4 g/cm^3, which is about half that of commonly used Ni-based superalloys), high-strength, and good oxidation resistance (Ref 1, 2).

When the alloys are utilized in high-temperature structures, cracks can be readily produced at geometric discontinuities, and consequently tearing failure under variable-amplitude load or overload can quickly occur. It has been commonly accepted until recently that notch strength results in notch sensitivity. Notch strength is a factor governing the safety of notch elements before crack initiation at the notch root, while fracture toughness is a factor governing safety after crack initiation at the notch root. The notch sensitivity of ultrafine-grained copper, cold-rolled Ni_3Al foils, polymethyl methacrylate glasses, Inconel 718, and low-carbon steels has been studied (Ref 3-8). Lukáš et al. (Ref 4) showed that the fatigue notch sensitivity of ultrafine-grained copper produced by the equal channel angular pressing technique was higher than that of standard polycrystalline copper. Cui et al. (Ref 5) examined the notch sensitivity of 95% cold-rolled Ni_3Al foils using double U-notched tensile specimens. The foils were found to be essentially insensitive to the presence of notches. Plastic deformation occurred locally at the notch root to relieve the stress concentration, resulting in the insensitivity of the notch. In Ref 7, the notch sensitivity of the Inconel 718 alloy was related to the concentration of the δ phase. The alloy exhibited no notch sensitivity when the amount of δ phase was higher than 0.62 wt.% ut showed strong notch sensitivity with an amount of δ phase smaller than 0.43 wt.%. Yu et al. (Ref 8) showed that the fracture of blades made of as-cast K418 superalloy occurred instantaneously by overheat damage, which reduced the strength of the interdendritic region. Internal defects in the blades, whether in the raw material or in the manufacturing or process defects, did not contribute to the fracture.

TiAl alloys are important intermetallic alloys for high-temperature structural applications because they can provide increased thrust-to-weight ratios and improved efficiency. The design methodology, finite element analysis, manufacturing techniques, material characterization, fracture mechanisms, toughening mechanisms, fatigue fracture process, and fatigue life of these alloys have been thoroughly investigated before their implementation into structural components (Ref 9-12). However, the tensile ductility of TiAl alloys is very low, and brittle interlamellar fracture and translamellar fracture dominate the fracture process (Ref 10-12). The tensile strength and tensile ductility at room temperature are affected by the alloy elements (Ref 13-15), lamellar colonies (Ref 9), lamellar orientation (Ref 16, 17), heat treatment (Ref 18), loading rate (Ref 19), testing temperature (Ref 20), and surface topography (Ref 21). In Ref 18), the heat-treated Ni-containing specimen exhibits superior tensile properties (yield strength of 445 MPa and elongation of 0.65%) compared to other specimens. The elimination of the bulk τ_3 phase, refined lamellar colonies, and lamellae spacing can account for the strengthening of the current heat-treated T4822-Ni specimen as well as for the ductility. In Ref 19), the ultimate tensile strength (UTS) and yield strength (YS) increased with increasing strain rate up to

R. Cao, J. X. Wen, and **J. H. Chen**, Department of Materials Science and Engineering, Lanzhou University of Technology, Lanzhou 730050, China; and State Key Laboratory of Advanced Processing and Recycling of Non-ferrous Metals, Lanzhou University of Technology, Lanzhou 730050, China; and **H. J. Liu**, Department of Materials Science and Engineering, Lanzhou University of Technology, Lanzhou 730050, China. Contact e-mail: caorui@lut.cn.

10/s. Specifically, in Ref 21), the authors indicated that the fracture behavior and tensile ductility of TiAl alloys are affected by the surface topography. Therefore, TiAl-based alloys, which are semi-brittle materials, are sensitive to the formation of notches and defects. Series studies indicated that various surface conditions have different effects on the fatigue properties of semi-brittle TiAl-based alloys (Ref 22-25). In Ref 26, various notch types have different effects on resistance to fatigue crack initiation, and the electropolishing of surfaces without defects can significantly improve the resistance to fatigue crack initiation of alloys. The fatigue life of specimens treated by electro-discharge machining (EDM) is indeterminate owing to the appearance of many holes and microcracks on the surface.

According to the above studies, the tensile ductility and fatigue life of TiAl alloys are also affected by the surface topography (Ref 21, 26) and other factors. Thus, to further understand the notch sensitivity or stress concentration behavior of K418 and TiAl alloys, the notch sensitivity of the two materials is systematically studied and compared in this study.

2. Materials and Experimental Procedures

A Ti-47.5Al-2.5V-1Cr alloy was used. All samples were taken from a forged pancake that was deformed at 1100 °C to a 70% height reduction. The samples were first inserted in a quartz tube, treated by hot isostatic pressing at 950 °C and 120 MPa in argon for 3 h, and then annealed at 1370 °C for 1 h, after which the corresponding fully lamellar (FL) TiAl microstructure was obtained (Fig. 1). The K418 material used in the investigation was prepared by casting. The nominal chemical composition of the material is Ni-12Cr-4Mo-6Al-2Nb-0.6Ti-0.1C-0.08Zr-0.01B. The microstructure of the K418 alloy is shown in Fig. 2. It is composed of four phases: a γ solid solution, a γ′ precipitated strengthening phase, MC-type carbide, and M_3B_2-type boride. The γ′ precipitated strengthening phase is dispersed in the γ matrix and is the main strengthening phase, which reaches 55% of the total weight. The γ–γ′ eutectic is distributed between grain boundaries and dendrites and accounts for 2% of the total weight. The MC-type carbide accounts for 1% of the total weight, and a small amount of M_3B_2-type boride is present in the K418 alloy. Figure 2(a) shows the metallurgical features obtained by etching with a typical dendritic pattern, and Fig. 2(b) shows the aciculae γ′ phase without etching.

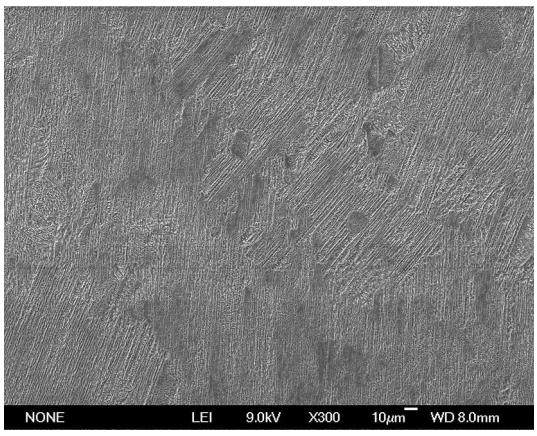

Fig. 1 Microstructure of the TiAl alloy

Standard notch rod tensile specimens, smooth rod tensile specimens, and special notch rod tensile specimens were machined, and the dimensions of the standard tensile and standard notch tensile specimens are shown in Fig. 3. Notch specimens with four different radii, 0.08, 0.13, 0.25, and 0.85 mm, were used. The dimensions of the special notch tensile specimens are shown in Fig. 4. Each special specimen contains eight machined 'cracks' of one single size produced by electro-discharge machining. Four different crack lengths/depths of 0.1, 0.5, 1, and 2 mm, were chosen to sample the complete grain size range. All tensile tests were carried out at ambient temperature (20 °C) and in laboratory air with the Instron test machine with a test speed of 1 mm/min. The load and displacement were recorded autographically.

The microstructure and fracture surface after the tensile tests were observed by means of scanning electron microscopy (JEOL-6700F).

3. Results and Discussions

3.1 Notch Sensitivity of Standard Rod Tensile Specimens

The engineering stress and strain curves of the specimens are shown in Fig. 5. The tensile strength of the smooth K418 specimen is much lower than that of the notch specimens, but the elongation is very high. However, for all notch specimens, the tensile strength increases and the elongation decreases as

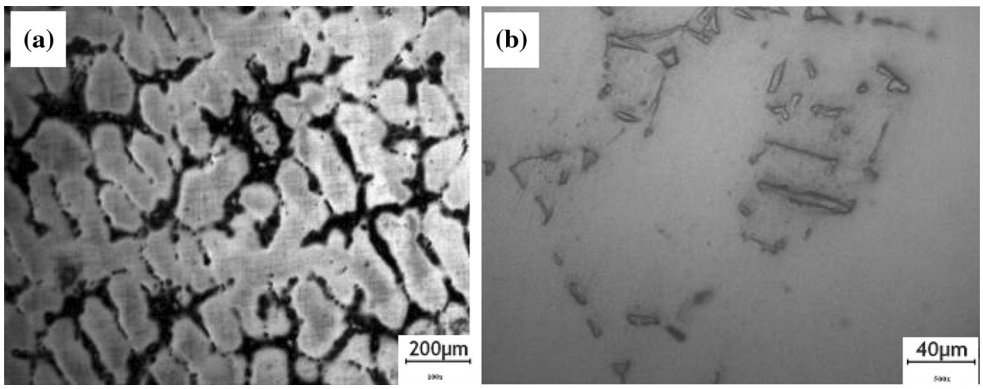

Fig. 2 Microstructure of the K418 alloy

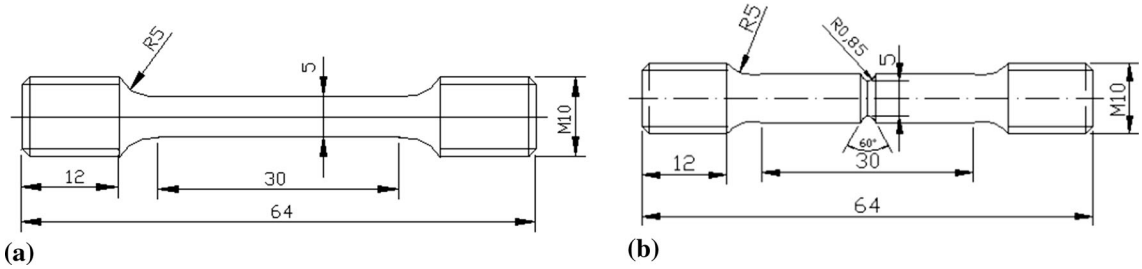

Fig. 3 Dimensions of the standard tensile and notch tensile specimens. (a) smooth rod tensile specimens and (b) standard notch tensile specimens

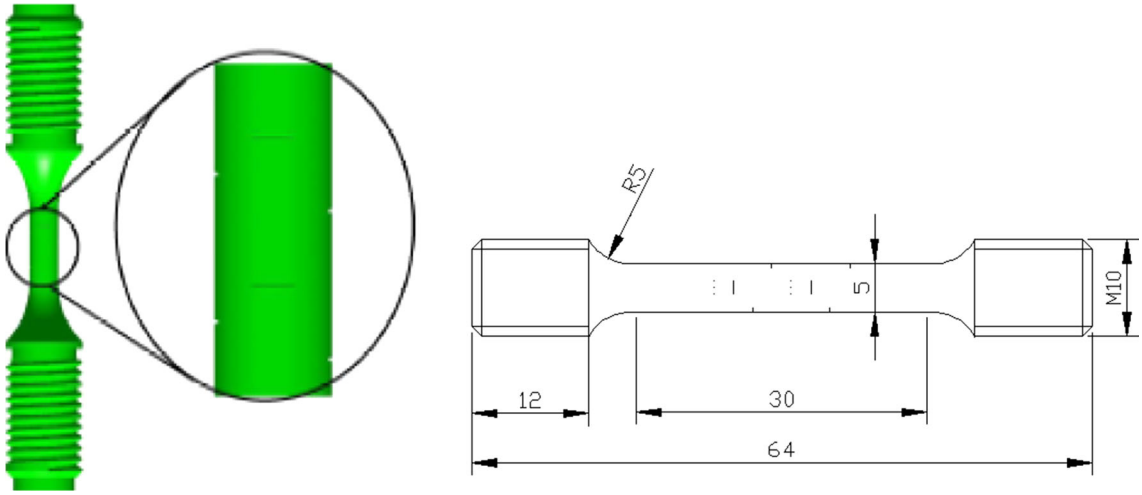

Fig. 4 Dimensions of the special notch tensile specimens

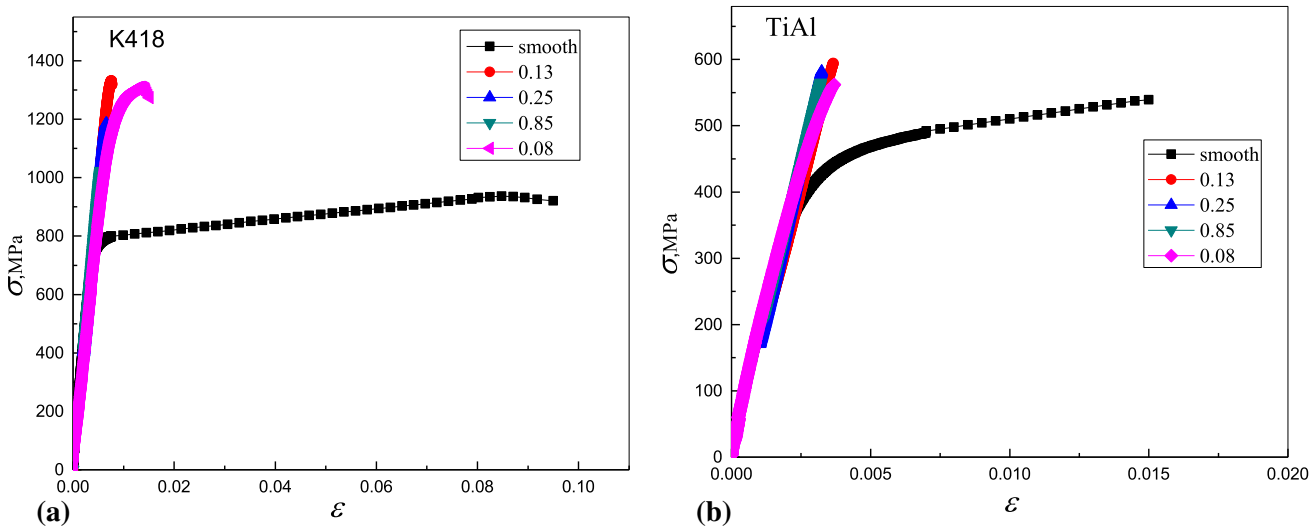

Fig. 5 Engineering stress–strain curves of the K418 (a) and TiAl (b) tensile specimens

the notch radius decreases. Plastic deformation is the only macroplastic behavior shown in the engineering stress and engineering strain curves. The tensile strength of the notch specimens is much higher than that of the smooth specimens, indicating that a higher notch strengthening effect occurs in the K418 specimen. However, for the TiAl specimen, a smaller tensile macroplastic is obtained even for smooth tensile specimens. The tensile strength of the notch specimens is also slightly higher than that of the smooth specimens.

The coefficient of stress concentration (K_t) and the notch sensitivity ratio (NSR) are calculated by $K_t = 1 + 2\sqrt{\frac{a}{\rho}}$ and

Table 1 Relationship between ρ–NSR–K_t

ρ	0.08 mm	0.13 mm	0.25 mm	0.85 mm	∞
K_t	8.07	6.55	5.00	3.17	
σ_b(TiAl) MPa	559.292	554.885	575.865	577.34	525.42
NSR(TiAl)	1.065	1.056	1.096	1.099	
σ_b(K418) MPa	1296.54	1331.80	1168.22	1023.29	865.615
NSR(K418)	1.496	1.539	1.350	1.182	

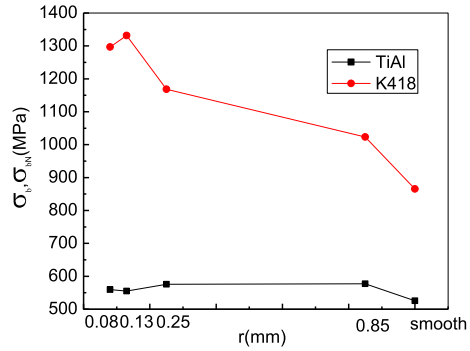

Fig. 6 Relationship between the tensile strength and notch radius

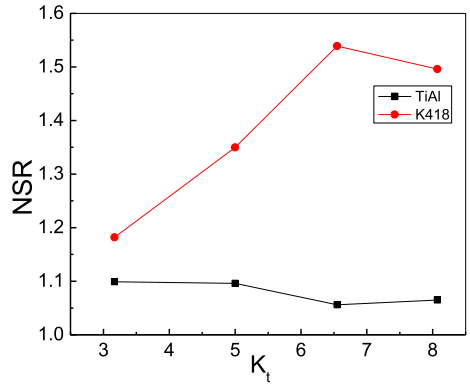

Fig. 7 Relationship between the NSR and K_t strength and the notch radius

NSR = $\frac{\sigma_{bN}}{\sigma_b}$, respectively, where a is the notch depth,ρ is the notch radius, σ_{bN} is the tensile strength of the notch specimen, and σ_b is the tensile strength of the smooth specimen. The notch sensitivity ratio (NSR) for different notch radii and the corresponding tensile strengths are listed in Table 1.

As seen in Fig. 5, the tensile strength (σ_{bN}) of the notch K418 specimens is very high, which is attributed to the high stress triaxiality of notch specimens, which in turn causes the yield stress to increase. Indeed, the yield stress is even higher than the tensile strength of smooth specimens. However, the true strain zone is very narrow and is restricted in the notch root, i.e., the fracture strain of the notch specimens is much lower than that of the smooth specimens. However, the fracture strength and tensile strength of the notch specimens are higher than that of the smooth specimens. If the notch sensitivity analysis is based on the definition of NSR, no obvious notch sensitivity appears in the K418 specimen because the tensile strength of the notch specimens is higher than that of the smooth specimens. Therefore, the lower fracture strain and higher fracture strength of the notch specimens are still induced by high stress triaxiality, which increases the yield stress.

Figure 6 and 7 show the relationships between the tensile strength, notch sensitivity ratio, and notch radius. From the combined data of Fig. 6, 7, and Table 1, it is found that the tensile strength of the notch specimens is higher than that of the smooth specimens, i.e., the nominal NSR is higher than 1 for the two materials. However, for the TiAl specimens, the NSR decreases with decreasing notch radius (increasing coefficient of stress concentration). For the K418 specimens, the NSR increases with decreasing notch radius (increasing coefficient of stress concentration). Therefore, the K418 alloy does not exhibit notch sensitivity, while the TiAl alloy exhibits small notch sensitivity. For the TiAl specimens, when the notch radius is smaller than 0.25 mm, the tensile strength decreases; therefore, a notch radius of 0.25 mm is a critical value.

In summary, based on the definition of the NSR, the K418 alloy is essentially insensitive to the presence of notches, while the TiAl alloy is slightly sensitive to the presence of notches.

3.2 Stress and Strain Distributions of Standard Rod Tensile Specimens

The stress and strain distribution in the front of a notch root varies with the notch radius and applied load in the K418 specimens. Various notch effects, such as stress concentration, strain concentration, and stress strengthening, arise in the notch specimens; thus, the final tensile strength also varies. To analyze the results in Table 1, the stress and strain distributions of the tensile specimens with different notch radii are calculated and are shown in Fig. 8. For a given notch radius, the maximum stress is distributed at a certain distance from the notch root. With increasing applied load, the maximum stress increases, the distance at which the maximum stress is distributed from the notch root decreases, and the maximum strain distributed at the notch root increases. The distribution of the stress triaxiality is similar to that of the stress.

The calculated results for different notch radii are shown in Fig. 9. At the same applied stress, the smaller the notch radius, the larger the maximum stress, maximum strain, and stress triaxiality of the specimens. To explain the fracture criterion, the stress and strain distributions of the K418 specimens with different notch radii are shown in Fig. 10. At the corresponding tensile strength, the smaller the notch radius, the higher the maximum stress and maximum stress triaxiality. However, for the K418 alloy, the maximum strain of the specimen with the smallest notch radius of 0.08 mm is slightly lower than that of the specimen with a notch radius of 0.13 mm. Moreover, cavities are formed and propagated in the second phase or carbide before fracture; therefore, plastic strain is the driving force of the fracture. Because higher stress triaxiality arises in specimens with smaller notch radii, it is difficult to produce yield deformation. Thus, a higher yield stress is needed to

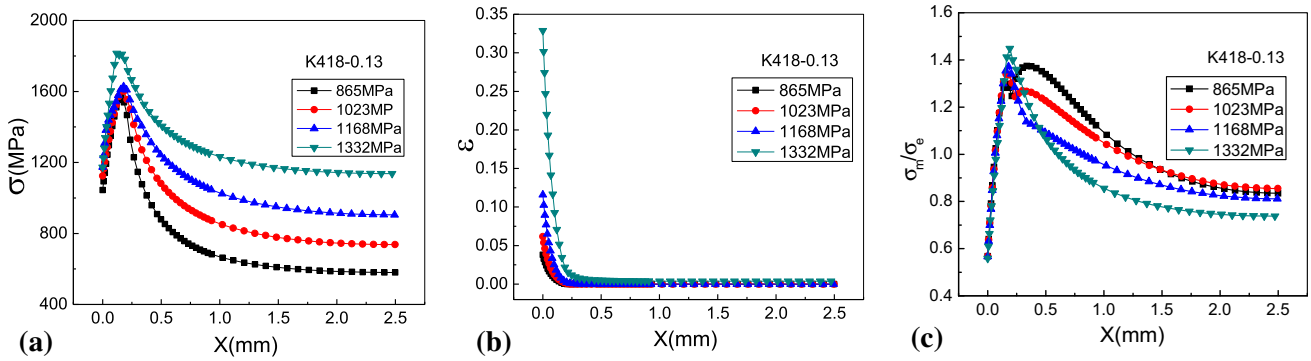

Fig. 8 Distribution of the stress (a), strain (b), and stress triaxiality (c) for the K418 specimens with a notch radius of 0.13 mm

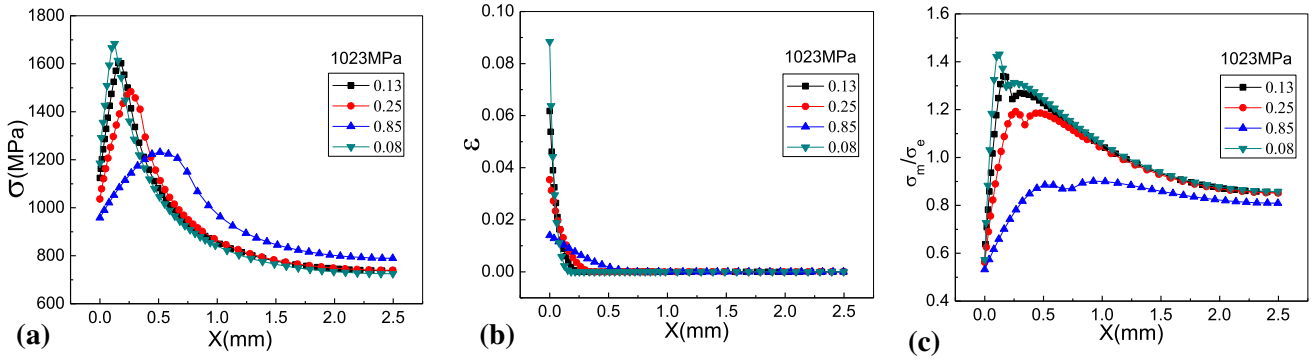

Fig. 9 Distribution of the stress (a), strain (b), and stress triaxiality (c) at the same applied stress for K418 specimens with different notch radii

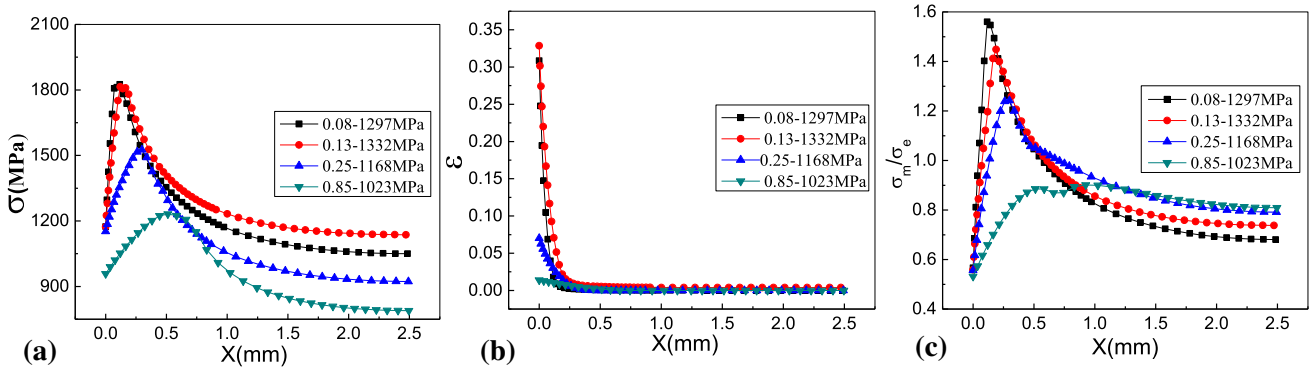

Fig. 10 Distribution of the stress (a), strain (b), and stress triaxiality (c) at the corresponding tensile strength for K418 specimens with different notch radii

produce the same deformation, and a higher tensile strength is obtained for the specimens with a smaller notch radius.

The strain distributions of various notch radii were also analyzed. For specimens with larger notch radii, the strain distributed at the center surface ahead of the notch root is very small, and the high strain is concentrated on the larger region ahead of the notch root. Therefore, the accumulated strain becomes very high. Figure 11 shows the strain distribution at the corresponding tensile strength for specimens with various notch radii. The maximum strain is very high for the specimen with the smallest notch radius, but as the range of high strain is very narrow, a higher applied load is needed to achieve the same deformation, and therefore a higher tensile strength is obtained. However, for the specimen with the largest notch radius, the maximum strain is very low but the range of high strain is very large, and therefore a smaller tensile strength is obtained. The statistical results of the strain are shown in Table 2; a similar statistical high strain zone ahead of the notch root is obtained for all K418 specimens with various notch radii at the corresponding tensile strength.

The NSR value of the K418 specimens is higher than 1. Therefore, it is concluded that K418 alloys are not sensitive to the presence of a notch, which is related to the measurement of the tensile strength. The notched tensile strength is obtained by the load divided by the area distributed at the cross section ahead of the notch root. With increasing notch radius, the stress and strain are not only concentrated on the cross section of the notch root but also on the larger region surrounding the notch. Therefore, according to the formula, a smaller area will lead to a higher tensile strength.

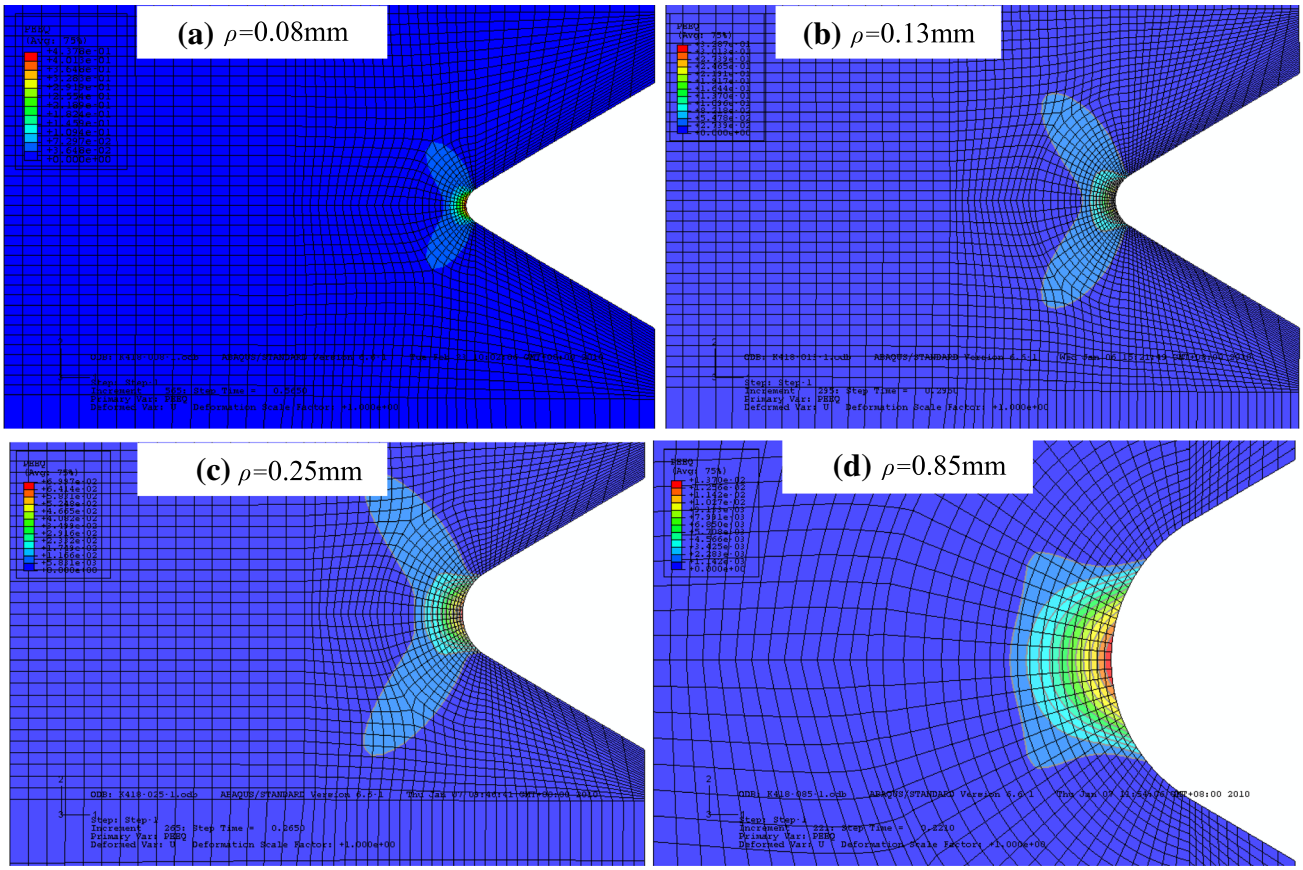

Fig. 11 Distribution of the strain at the corresponding tensile strength for K418 specimens with different notch radii

Table 2 Statistical results of the high strain zone at the corresponding tensile strength for K418 specimens with different notch radii

Radius (mm)	0.08	0.13	0.25	0.85
Areas of high strain zone (mm^2)	0.29	0.303	0.473	0.592

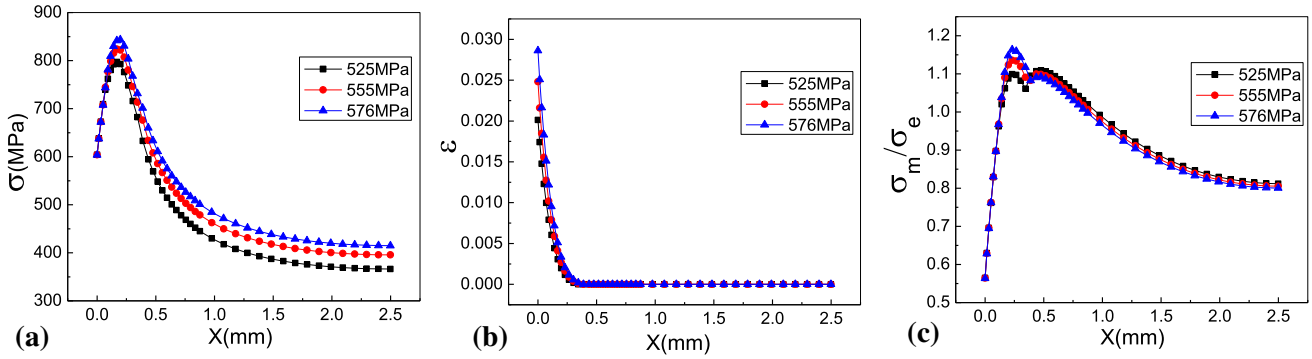

Fig. 12 Distribution of the stress (a), strain (b), and stress triaxiality (c) for K418 specimens with a notch radius of 0.25 mm

The stress, strain, and stress triaxiality distributions of notched specimens of TiAl at various applied loads are also calculated and shown in Fig. 12. The trends are similar to those in Fig. 8 with the maximum stress distributed at a certain distance from the notch root. With increasing applied load, the maximum stress increases, the distance at which the maximum stress is distributed from the notch root decreases, and the maximum strain distributed at the notch root increases. The distribution of the stress triaxiality is similar to that of the stress.

A higher tensile strength is obtained for the TiAl notched specimens, which is attributed to a higher yield stress, but the TiAl specimens are fractured at a lower fracture stress—even

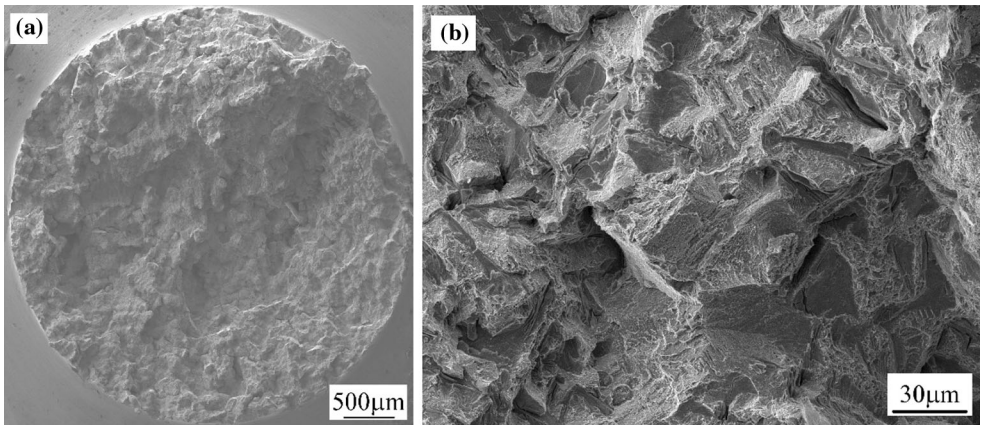

Fig. 13 Fracture surface of K418 alloys

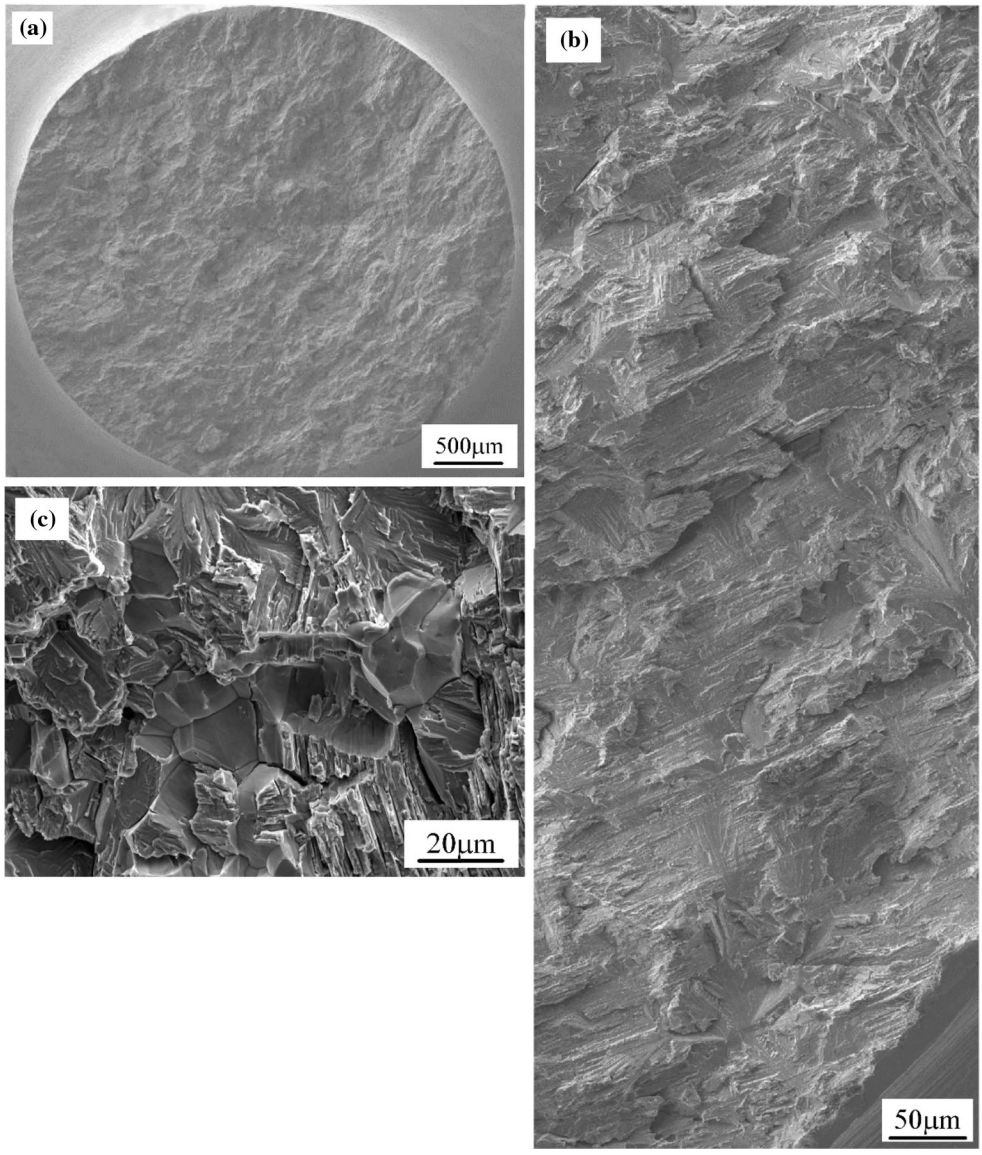

Fig. 14 Fracture surface of TiAl alloys with 0.85 μm of notch radius

lower than the yield stress, and the fractures are propagated at a low plastic strain. Thus, the normal stress σ_{yy} at the corresponding applied tensile strength is the same for all specimens.

According to several studies, normal stress is the driving force of fracture, and typical brittle fracture dominates the fracture mode of specimens (Ref 11). Thus, for the specimen with the smallest notch radius, a higher coefficient of stress concentration appears on the notch root, and the specimen is fractured at a lower applied load to achieve the same resistance, i.e., a smaller notch tensile strength is produced.

In summary, no notch sensitivity is produced in the K418 alloy, and the final fracture of the K418 specimens is controlled by strain and not by stress. A smaller strain is distributed ahead of the notch root for specimens of larger notch radii, but as the region of high strain becomes wider, the accumulated strain

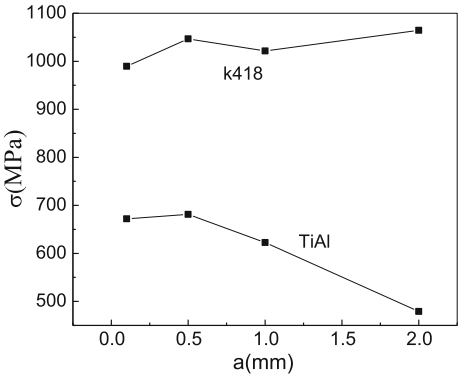

Fig. 16 Relationship between the tensile strength and notch radius

Table 3 Tensile results of special specimens

	A (mm^2)	E (Gpa)	σ_b (MPa)	σ_f (MPa)	ε_f (%)
TiAl-∞	19.650	162.439	525.420	525.420	1.5
TiAl(2)	11.076		478.967		0.411
TiAl(1)	13.839		622.682		0.435
TiAl(0.5)	15.613		681.317		0.835
TiAl(0.1)	17.861		671.972		1.490
K418(∞)	19.635	205.940	936.475	921.019	9.5
K418(2)	11.076		1064.64		1.411
K418(1)	13.839		1021.57		1.33
K418(0.5)	15.613		1046.85		3.084
K418(0.1)	17.861		989.675		6.526

A area of fracture surface, E elastic modulus, σ_f macrofracture stress, ε_f macrofracture strain, σ_b tensile strength

Table 4 Relationship between ρ–K_t–σ_b–NSR

ρ K_t	0.1 mm 3	0.5 mm 5.47	1 mm 7.32	2 mm 9.94	∞
σ_b(TiAl) MPa					525.420
σ_{bN}(TiAl) MPa	671.972	681.317	622.682	478.967	
NSR(TiAl)	1.279	1.297	1.185	0.912	
σ_b(K418) MPa					936.475
σ_{bN}(K418) MPa	989.675	1046.85	1021.57	1064.64	
NSR(K418)	1.057	1.118	1.091	1.137	

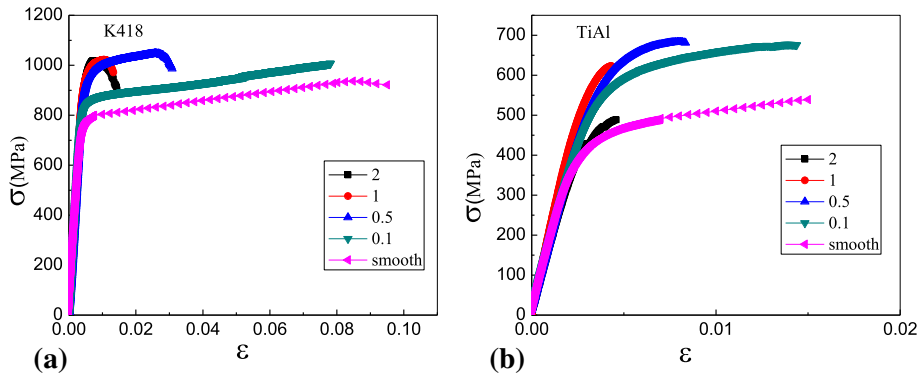

Fig. 15 Engineering stress–strain curves of the tensile specimens

becomes higher, and a lower applied tensile strength is obtained. The notch tensile strength increases with decreasing notch radius as the stress strengthening effects and higher yield strength are induced by stress triaxiality. The NSR of all the specimens with various notch radii is higher than 1, and therefore the K418 alloy does not exhibit notch sensitivity.

Figure 13 and 14 show the fracture surface of TiAl and K418 specimens, respectively. Ductile fracture (tear ridge) and dendritic fracture dominate the fracture surface of the K418 specimens, while quasi-cleavage fractures including interlamellar fracture and translamellar fracture dominate the fracture surface of the TiAl specimens. As the basic nature of the two materials is different, the driving force of fracture and fracture inertia are also different for the brittle TiAl alloy and ductile K418 alloy, which results in the different notch sensitivity level, i.e., K418 does not exhibit notch sensitivity, while TiAl exhibits small notch sensitivity.

As seen in Fig. 6 and 7, the smaller the notch ratio, the larger the NSR, and when the notch radius is larger than 0.85 mm, no sensitivity arises, even in the TiAl alloy.

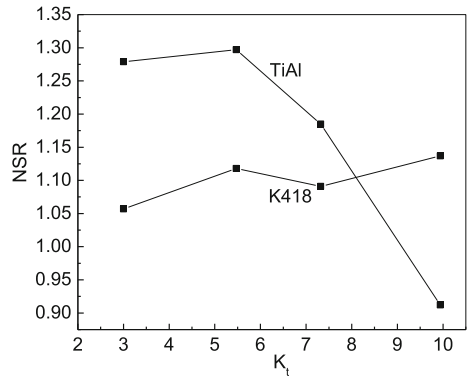

Fig. 17 Relationship between the *NSR* and K_t

3.3 Notch Sensitivity of Special Notch Rod Tensile Specimens

The notch sensitivity ratio is generated from Table 3 using a specifically designed defect sensitivity test specimen.

The coefficient of stress concentration (K_t) and the notch sensitivity ratio (NSR) are calculated by $k_t = 1+2\sqrt{\frac{a}{\rho}}$ and $NSR = \frac{\sigma bN}{\sigma b}$, respectively, where a is the notch depth and ρ is the notch radius. The corresponding results are shown in Table 4.

As seen in Fig. 15, the tensile strength (σ_{bN}) of the notch specimens of K418 is very high and is attributed to the high stress triaxiality of notch specimens, which causes the yield stress to increase; the yield stress is even higher than the tensile strength of smooth specimens. If the notch sensitivity analysis is based on the definition of the NSR, no obvious notch

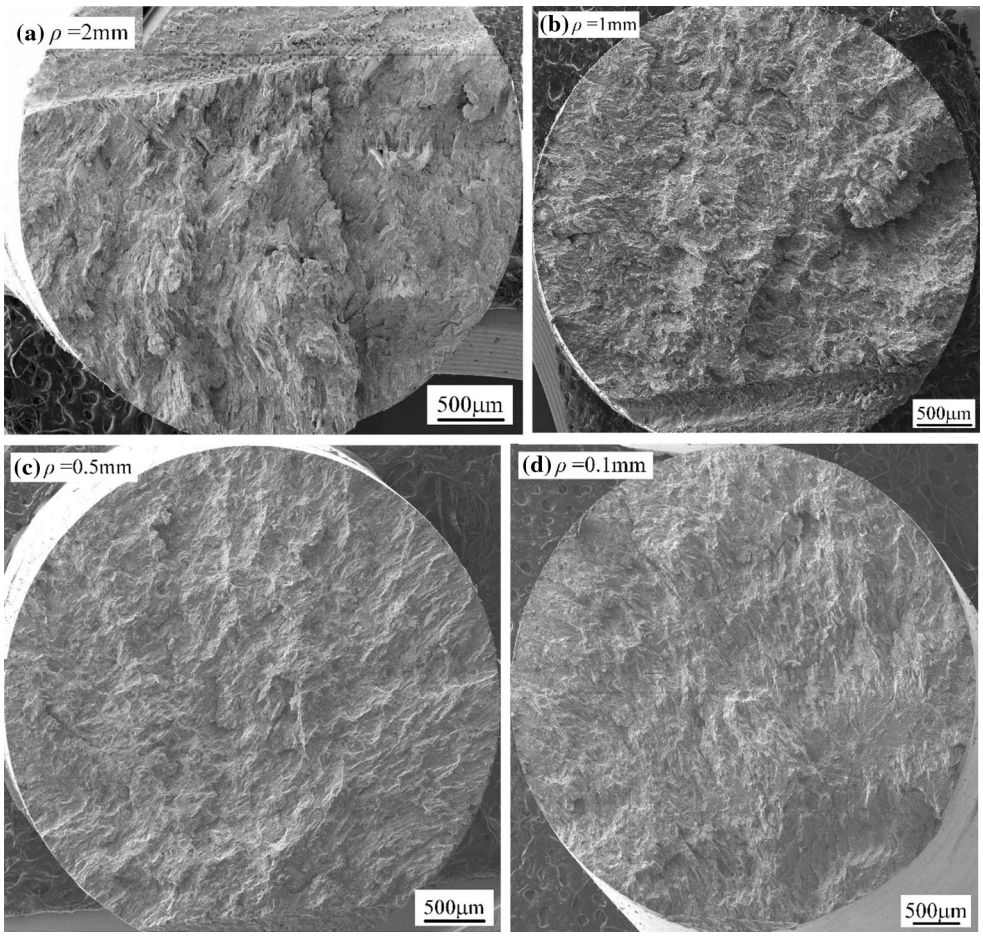

Fig. 18 Fracture surface of tensile specimens with different notch depth for TiAl alloys

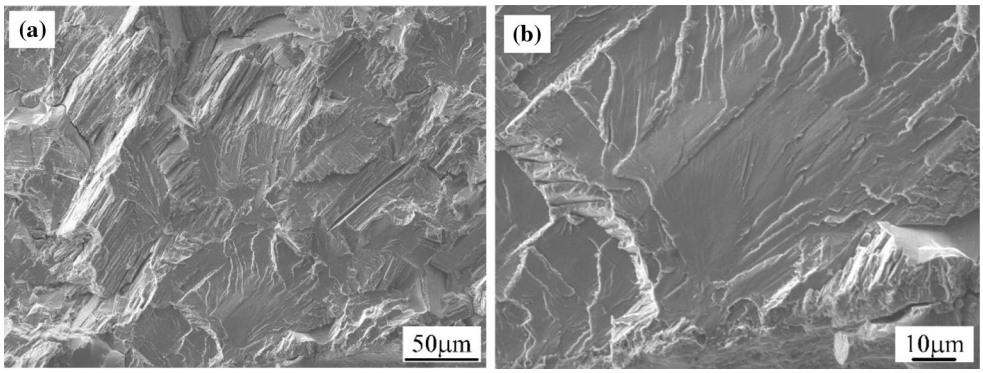

Fig. 19 Feature of initiation origins of tensile specimens with 0.5 mm of notch depth for TiAl

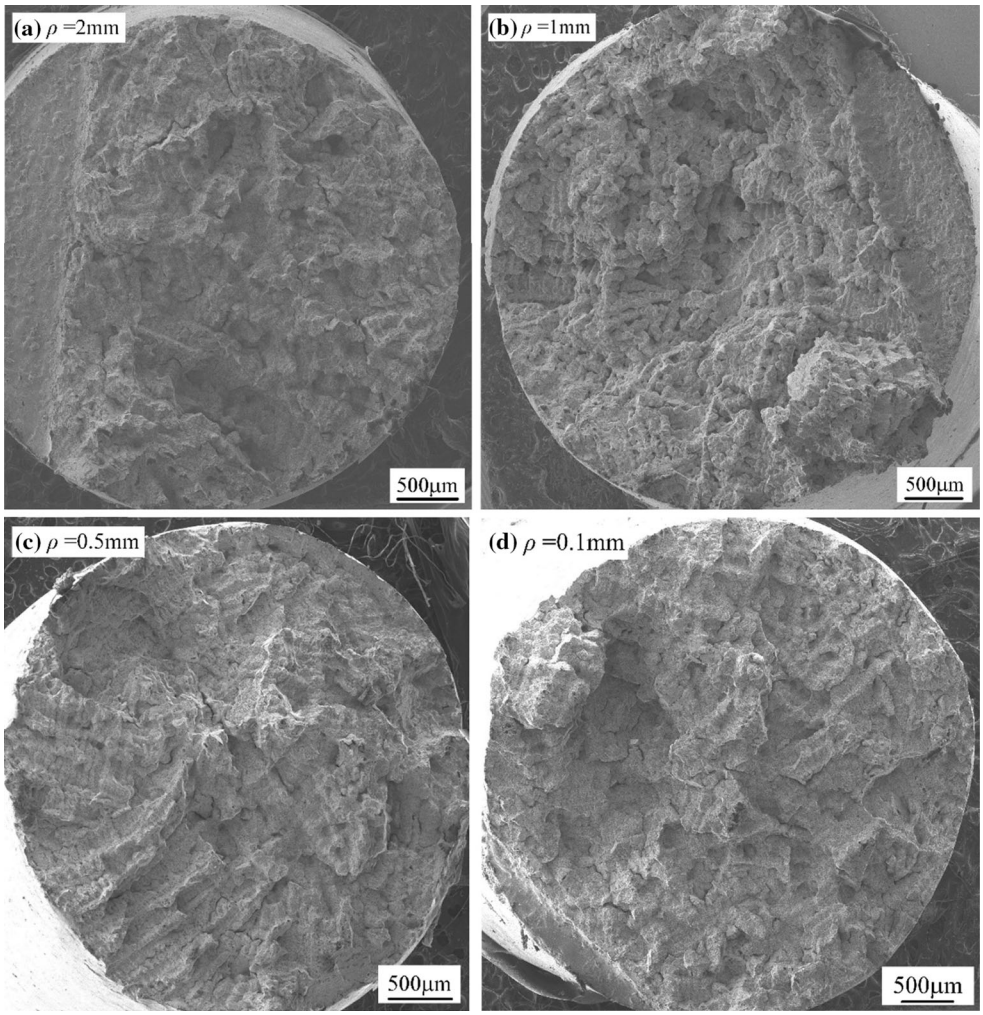

Fig. 20 Fracture surface of tensile specimens with different notch depth for K418 alloys

sensitivity appears in the K418 specimens because the tensile strength of notch specimens is higher than that of smooth specimens. The lower fracture strain and higher fracture strength of notch specimens are still induced by stress triaxiality, which increases the yield stress. For TiAl specimens, the tensile strength (σ_{bN}) of notch specimens with 0.1, 0.5, and 1 mm notch depths is very high. However, for the specimen with a 2-mm notch depth, a low notch tensile strength, lower than that of the smooth specimen, is obtained.

Figure 16 and 17 show the relationships between the notch depth, coefficient of stress concentration, notch sensitivity ratio, and notch strength. The K418 alloy does not exhibit notch sensitivity. Until the notch depth reaches 2 mm, there is no obvious declining trend in the fracture strength of the K418

specimens. However, for the TiAl specimens, the tensile strength decreases when the notch depth reaches 0.5 mm. The tensile strength decreases to 25% of the tensile strength of smooth specimens when the notch depth increases from 1 mm to 2 mm. When the notch depth reaches 10% of the specimen diameter, the tensile strength decreases; when the notch depth reaches 20% of the specimen diameter, the tensile strength decreases sharply. Therefore, these parameters can be regarded as important to estimate the notch depth or depth of casting defect.

The fracture surface of special rod tensile specimens of the two materials was also analyzed. Although eight surface cracks located in different cross sections and a symmetrical stress distribution were considered, the final fracture still occurred at one section of a given notch root. The coefficient of stress concentration increases with increasing notch depth. Therefore, the maximum coefficient of stress concentration and the largest stress of notch root were obtained for the TiAl specimen with the largest notch depth. The driving force of fracture will be reached and fracture will occur at a lower applied load, and thus the nominal notch strength is smaller. As seen in Fig. 18 and 19, a coarse fracture surface appears with increasing notch depth, and more translamellar fractures dominate the fracture surface. For the specimen with a 0.5-mm notch depth, cleavage fracture is induced by interlamellar cracking origins (Fig. 19). Figure 20 shows the fracture surface of the K418 specimens. The fracture surface of the special rod tensile specimen is the same as that of the rod tensile specimen. Tear ridge and dendritic fracture control the fracture surface.

4. Conclusions

Based on the test results and analysis of the notch strength of K418 and TiAl specimens, the following preliminary conclusions can be drawn:

1. Ductile fracture (tear ridge) and dendritic fracture dominate the fracture surface of the K418 specimens, while quasi-cleavage fractures including interlamellar fracture and translamellar fracture dominate the fracture surface of the TiAl specimens.
2. The basic nature of the two materials is different, and thus the driving force of fracture and the fracture criteria are also different for the brittle TiAl alloy and the ductile K418 alloy. The final fracture of the K418 specimens is controlled by strain and not by stress, and K418 does not exhibit notch sensitivity. However, the final fracture of the TiAl specimens is controlled by stress, and TiAl exhibits small notch sensitivity.
3. Notch sensitivity still does not arise in special notch rod tensile K418 specimens. Until the notch depth reaches 2 mm, there is no obvious declining trend in the fracture strength of the K418 specimens. However, for the TiAl specimens, the tensile strength decreases when the notch depth reaches 0.5 mm, and when the notch depth increases from 1 to 2 mm, the tensile strength decreases to 25% of the tensile strength of smooth specimens. When the notch depth reaches 10% of the specimen diameter, the tensile strength decreases. When the notch depth reaches 20% of the specimen diameter, the tensile strength decreases sharply. These parameters are regarded as important to estimate the notch depth or depth of casting defect.

Acknowledgments

This work was financially supported by the National Nature Science Foundation of China (Nos. 51761027, 51675255), the Program of Innovation Groups of Basic Research of Gansu Province (17JR5RA107), and the Foundation of Collaborative Innovation Teams in College of Gansu Province (2017C-07). The authors wish to express their appreciation to Mr. Edmund and Ms. Li Shuxin for their help in English editing. The authors also wish to thank the editors and reviewers for their comments and suggestions.

References

1. M.T. Jovanovic, B. Dimcic, I. Bobic, S. Zec, and V. Maksimovic, Microstructure and Mechanical Properties of Precision Cast TiAl Turbocharger Wheel, *J. Mater. Process. Technol.*, 2005, **167**, p 14-21
2. T. Tetsui and S. Ono, Endurance and Composition and Microstructure Effects on Endurance of TiAl Used in Turbochargers, *Intermetallics*, 1999, **7**(6), p 689-697
3. W.D. Pilkey, *Peterson's Stress Concentration Factors*, Wiley Interscience Publication, New York, 1997
4. P. Lukáš, L. Kunz, and M. Svoboda, Fatigue Notch Sensitivity of Ultrafine-Grained Copper, *Mater. Sci. Eng., A*, 2005, **391**, p 337-341
5. C.Y. Cui, M. Demura, K. Hasegawa, T. Ohashi et al., Notch Sensitivity of Heavily Cold-Rolled Ni3Al Foils, *Scr. Mater.*, 2005, **53**, p 1339-1343
6. X.L. Zheng, H. Wang, and J.H. Yan, Notch Strength and Notch Sensitivity of Polymethyl Methacrylate Glasses, *Mater. Sci. Eng., A*, 2003, **349**, p 80-88
7. D.Y. Cai, W.H. Zhang, P.L. Nie, W.C. Liu, and M. Yao, Dissolution Kinetics of δ Phase and Its Influence on the Notch Sensitivity of Inconel 718, *Mater. Charact.*, 2007, **58**, p 220-225
8. Z.W. Yu, X.L. Xu, S.H. Liu, and Y. Li, Failure Investigation on Failed Blades Used in a Locomotive Turbocharger, *J. Fail. Anal. Prev.*, 2007, **7**, p 386-392
9. P. Wang, N. Bhate, K.S. Chan et al., Colony Boundary Resistance to Crack Propagation in Lamellar Ti-46Al, *Acta Mater.*, 2003, **51**(6), p 1573-1591
10. J.H. Chen, R. Cao, J. Zhang, and G.Z. Wang, Fracture Behaviour of Precracked Specimens of a TiAl alloy, *Mater. Sci. Technol.*, 2005, **21**(5), p 507-516
11. J.H. Chen, R. Cao, G.Z. Wang, and J. Zhang, Study on Notch Fracture of TiAl Alloys at Room Temperature, *Metall. Mater. Trans. A*, 2004, **35A**(2), p 439-457
12. K.S. Chan, P. Wang, N. Bhate, and K.S. Kumar, Intrinsic and Extrinsic Fracture Resistance in Lamellar TiAl Alloys, *Acta Mater.*, 2004, **52**, p 4601-4614
13. V. Recina, D. Lundström, and B. Karlsson, Tensile, Creep, and Low-Cycle Fatigue Behavior of a Cast γ-TiAl-Based Alloy for Gas Turbine Applications, *Metall. Mater. Trans. A*, 2002, **33**(9), p 2869-2881
14. E. Hamzah, M. Kanniah, and M. Harun, Effect of Chromium Addition on Microstructure, Tensile Properties and Creep Resistance of As-cast Ti-48Al Alloy, *J. Mater. Sci.*, 2007, **42**(21), p 9063-9069
15. D. Hu, Role of Boron in TiAl Alloy Development: A Review, *Rare Met.*, 2016, **35**(1), p 1-14
16. H. Inui, M.H. Oh, A. Nakamura, and M. Yamaguchi, Room-Temperature Tensile Deformation of Polysynthetically Twinned (PST) Crystals of TiAl, *Acta Mater.*, 1992, **40**(11), p 3095-3104
17. F. Min, Y. Hong, Y. Ma, and S. Li, Experiments and Analyses on Tensile Behaviour of a TiAl Alloy with Lamellar Structure, *J. Mater. Sci.*, 2000, **35**(19), p 4937-4943
18. J.C. Han, S.L. Xiao, J. Tian, Y.Y. Chen, L.J. Xu, X.P. Wang et al., Microstructure Characterization and Tensile Properties of a Ni-Containing TiAl-Based Alloy with Heat Treatment, *Rare Met.*, 2016, **35**(1), p 26-34
19. Z.M. Sun, T. Kobayashi, H. Fukumasu, I. Yamamoto, and K. Shibue, Tensile Properties and Fracture Toughness of a Ti-45Al-1.6Mn Alloy at Loading Velocities of up to 12 m/s, *Metall. Mater. Trans. A*, 1998, **29**(1), p 263-277
20. V.N. Nadakuduru, D.L. Zhang, B. Gabbitas, and Y.L. Chiu, Tensile Properties and Fracture Behaviour of an Ultrafine Grained Ti-47Al-2Cr

(at.%) Alloy at Room and Elevated Temperatures, *J. Mater. Sci.*, 2012, **47**(3), p 1223-1233
21. B. Lin, R. Liu, Q. Jia, Y. Cui, and R. Yang, Effect of Surface Topography on Room Temperature Tensile Ductility of TiAl, *JOM*, 2017, **69**, p 2583-2587
22. R. Botten, X. Wu, D. Hu, and M.H. Loretto, The Significance of Acoustic Emission During Stressing of TiAl-Based Alloys. Part I: Detection of Cracking During Loading Up in Tension, *Acta Mater.*, 2001, **49**(10), p 1689
23. G. Hénaff and A.L. Gloanec, Fatigue Properties of TiAl Alloys, *Intermetallics*, 2005, **13**(5), p 553
24. D. Novovic, R.C. Dewes, D.K. Aspinwall, W. Voice, and P. Bowen, The Effect of Machined Topography and Integrity on Fatigue Life, *Int. J. Mach. Tools Manuf*, 2004, **44**(2), p 131
25. S. Bolz, M. Oehring, J. Lindemann, F. Pyczak, J. Paul, A. Stark, and S. Weiß, Microstructure and Mechanical Properties of a Forged β-Solidifying γ-TiAl Alloy in Different Heat Treatment Conditions, *Intermetallics*, 2015, **58**(1), p 79
26. Z.-J. Yang, H.-L. Sun, Z.-W. Huang, X.-S. Jiang, and S. Chen, Fatigue Properties of a Medium-Strength g-TiAl Alloy with Different Surface Conditions, *Rare Met.*, 2016, **35**(1), pp 93-99